JOURNAL OF SOLID STATE CHEMISTRY 102, 570–574 (1993)

Synthesis and Magnetic Properties of $(Mg_{6-x}Al_x)MnO_8$ $(0 \leq x \leq 0.3)$

HIDEKI TAGUCHI,[1] AKIHIRO OKAMOTO, AND MAHIKO NAGAO

Research Laboratory for Surface Science, Faculty of Science, Okayama University, Okayama 700, Japan

AND HIROYASU KIDO

Osaka Municipal Technical Institute, Jyoto-ku, Osaka 536, Japan

Received May 11, 1992; in revised form July 20, 1992; accepted July 21, 1992

Murdochite-type $(Mg_{6-x}Al_x)MnO_8$ $(0 \leq x \leq 0.3)$ was synthesized at 1073 K using a solid state reaction. The cell constants of $(Mg_{6-x}Al_x)MnO_8$ monotonously decrease with increasing x. From the results of the magnetic measurement, both low-spin and high-spin states of Mn^{3+} ions coexist. The binding energy of Mn $2p_{3/2}$ determined from XPS measurement is independent of the composition. But the full width at half maximum (FWHM) of the Mn $2p_{3/2}$ peak increases with increasing x. The presence of both low-spin and high-spin states of the Mn^{3+} ion causes an increase of the FWHM of the Mn $2p_{3/2}$ peak.

Introduction

The crystal structure of murdochite-type Mg_6MnO_8 is cubic with $a = 0.8381 \pm 0.0002$ nm and space group $Fm3m$ (*1*). Mg_6MnO_8 is considered to be derived from the rock-salt structure of MgO by replacement of one-eighth of the Mg^{2+} ions with Mn^{4+} ions and one-eighth with vacancies. Mn^{4+} ions and vacancies occupy (111) alternate lattice layers and are ordered within the layers. Both Mg^{2+} and Mn^{4+} ions are octahedrally coordinated by six oxygen ions (*2*).

Mg_6MnO_8 is generally synthesized at high temperature (over 1173 K) in the flow of oxygen gas using a solid state reaction. Although the molar ratio of Mg/Mn in the starting materials was stoichiometric (6/1), the X-ray powder diffraction pattern shows that the sample fired at high temperature is a mixture of Mg_6MnO_8 and MgO (*1*, *2*). For this reason, excess magnesium oxide or magnesium acetate is generally used to synthesize Mg_6MnO_8 (the molar ratio of Mg/Mn $> 6/1$), and excess MgO in the sample is removed by washing with a hot 10% solution of NH_4Cl. By using a sol–gel process, Taguchi *et al.* synthesized Mg_6MnO_8 from the stoichiometric molar ratio of Mg/Mn (*3*).

Porta and Valigi measured the magnetic susceptibility of Mg_6MnO_8 in the temperature range 98–294 K (*2*). Mg_6MnO_8 has a weak antiferromagnetic interaction with paramagnetic Curie temperature (T_θ) $= -20 \pm 5$ K. The effective magnetic moment (μ_{eff}) in the paramagnetic region is 3.94 ± 0.08

[1] To whom correspondence should be addressed.

0022-4596/93 $5.00

μ_B, and this value agrees with the spin-only value calculated for a $3d^3$ ion in the octahedral configuration (3.87 μ_B).

Cimino and Indovina measured the catalytic activity of Mg_6MnO_8 and α-Mn_2O_3 for N_2O decomposition (*4*). Although Mg_6MnO_8 can decompose N_2O, the catalytic activity of Mg_6MnO_8 is lower than α-Mn_2O_3. This result shows that Mn^{3+} ions are more active in N_2O decomposition than Mn^{4+} ions.

In the present study, we tried to synthesize $(Mg_{6-x}Al_x)MnO_8$ at low temperature using the solid state reaction. As the valence of Al ions is 3+, $(Mg_{6-x}Al_x)MnO_8$ has a mixed valence of Mn (3+ and 4+) and the ratio of Mn^{3+}/Mn^{4+} changes linearly with increasing x. From crystallographic, magnetic, and X-ray photoelectron spectroscopy (XPS) measurements, we made clear the electron configurations of both Mn^{4+} and Mn^{3+} ions. These results provide some information for improving the catalytic activity of Mg_6MnO_8 in N_2O decomposition.

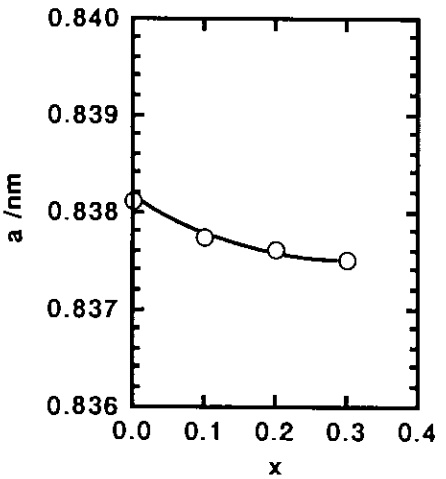

FIG. 1. Cell constant vs composition for the system $(Mg_{6-x}Al_x)MnO_8$.

Experimental

$(Mg_{6-x}Al_x)MnO_8$ ($0 \leq x \leq 0.3$) was synthesized by solid state reaction. Powders of $Mg(CH_3COO)_2 \cdot 4H_2O$, $Al_2O(CH_3COO)_2 \cdot 4H_2O$, and $Mn(CH_3COO)_2 \cdot 4H_2O$ were weighed in the proper proportions and milled with acetone. After the mixed powders were dried at 373 K, they were calcined at 673 K for 6 hr in a flow of pure oxygen gas. Then they were fired at 873 K for 6 hr, at 973 K for 6 hr, and finally at 1073 K for 6 hr in a flow of pure oxygen gas.

The phases of the samples were identified by X-ray powder diffraction with monochromatized Cu$K\alpha$ radiation. The cell constants of the samples were determined from high-angle radiation with Si as a standard.

The magnetic susceptibility was measured by a magnetic torsion balance in the temperature range 80 to 550 K. XPS measurement was carried out for the Mg 2*s*, Mn 2*p*, and O 1*s* levels of the samples using Mg $K\alpha$ radiation at room temperature. The energy calibration was made against the C 1*s* peak from the usual contamination.

Results and Discussion

X-ray powder diffraction patterns of $(Mg_{6-x}Al_x)MnO_8$ ($0 \leq x \leq 0.3$) were completely indexed as a murdochite-type structure. As $(Mg_{6-x}Al_x)MnO_8$ was synthesized below 1073 K, we could not find MgO at all. In the range $x > 0.3$, the samples had both murdochite-type oxide peaks and extra peaks. The relation between the cell constants and the composition is shown in Fig. 1. The cell constants decrease monotonously with increasing x. The coordination number of Mg^{2+}, Al^{3+}, Mn^{4+}, and Mn^{3+} ions is 6, because $(Mg_{6-x}Al_x)MnO_8$ is derived from the rock-salt structure. The ionic radii of Mg^{2+}, Al^{3+}, Mn^{4+}, Mn^{3+} (low-spin state), and Mn^{3+} (high-spin state) ions are 0.072, 0.053, 0.054, 0.058, and 0.065 nm, respectively (*5*). We calculated the rate of increase for the ionic radius of $(Mg_{6-x}Al_x)MnO_8$ as follows. Equations (1)–(3) are for the Mg site and for two Mn-sites (Mn^{4+} and low-

spin state of Mn^{3+} ions, Mn^{4+} and high-spin state of Mn^{3+} ions), respectively:

$$(r_{Mg^{2+}} - r_{Al^{3+}})/r_{Mg^{2+}} = -26.4\% \quad (1)$$

$$(r_{Mn^{4+}} - r_{Mn^{3+}\,(\text{low-spin state})})/r_{Mn^{4+}} = 7.4\% \quad (2)$$

$$(r_{Mn^{4+}} - r_{Mn^{3+}\,(\text{high-spin state})})/r_{Mn^{4+}} = 20.4\%. \quad (3)$$

In these equations, r is the ionic radius. Though the rate of increase for the Mn site is positive, the absolute value for the Mn site is smaller than that for the Mg site. From these results, the monotonic decrease of the cell constants is explained by the difference in the rate of increase for the ionic radii of the Mg site and the Mn site.

The magnetic susceptibility (χ) of $(Mg_{6-x}Al_x)MnO_8$ was measured in the temperature range from 80 to 550 K. $(Mg_{6-x}Al_x)$-MnO_8 is antiferromagnetic with paramagnetic Curie temperature (T_θ) = -23 ± 6 K. T_θ is independent of the composition. The $1/\chi$-T curves for $0 \leq x \leq 0.3$ are linear and follow the Curie–Weiss law. We calculated the effective magnetic moment (μ_{eff}) from the linear portion of the $1/\chi$-T curves. Figure 2 shows the relation between μ_{eff} and the composition. In Fig. 2 the open circles indicate the observed μ_{eff}. The observed μ_{eff} for $x = 0$ is 3.87 ± 0.05 μ_B and is nearly equal to the value reported by Porta and Valigi (*2*). The observed μ_{eff} is independent of the composition. Mn^{4+} ions ($3d^3$) have only one type of electron configuration with $(d\varepsilon)^3(d\gamma)^0$. On the other hand, Mn^{3+} ions ($3d^4$) have two types of electron configuration: One is the low-spin state with $(d\varepsilon)^4(d\gamma)^0$, and the other is the high-spin state with $(d\varepsilon)^3(d\gamma)^1$. Lines 1, 2, and 3 are drawn for the theoretical values calculated under the following assumptions of the spin state of Mn^{3+} ions: Line 1 is for the high spin-state of Mn^{3+}, line 2 is for the low spin-state of Mn^{3+}, and line 3 is for the coexistence of the low-spin and high-spin states of Mn^{3+} ions. As seen in Fig. 2, the observed μ_{eff} agree with line 3. According to Raccah and Goodenough, both the low-spin and high-spin states of Co^{3+} ions coexist in the perovskite-type $LaCoO_3$ (*6*). The ratio of the low-spin and high-spin states of Co^{3+} ions changes with increasing temperature.

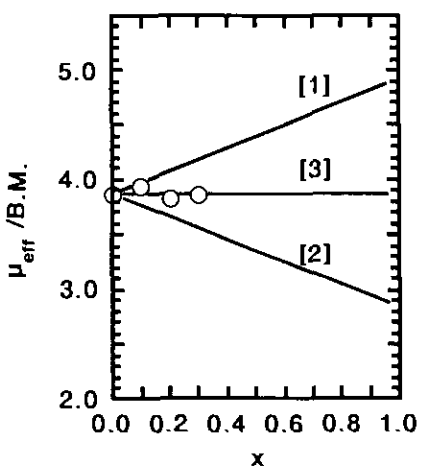

FIG. 2. Effective magnetic moment vs composition for the system $(Mg_{6-x}Al_x)MnO_8$. Line 1 is for the high spin-state of Mn^{3+}, line 2 is for the low spin-state of Mn^{3+}, and line 3 is for the coexistence of the low-spin and high-spin states of Mn^{3+} ions.

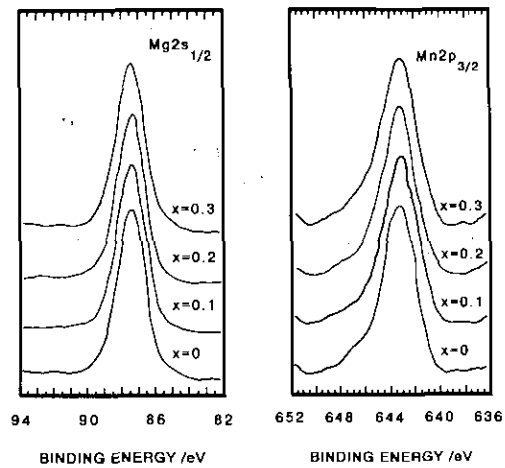

FIG. 3. XPS spectra of the Mg 2*s* and Mn 2*p* levels for the system $(Mg_{6-x}Al_x)MnO_8$.

Therefore, the coexistence of the low-spin and high-spin states of the Mn^{3+} ions in $(Mg_{6-x}Al_x)MnO_8$ is not unusual.

Taguchi and Shimada measured the XPS of perovskite-type $CaMnO_{3-\delta}$ and $(Ca_{1-x}La_x)MnO_{2.97}$ and discussed the chemical bonding of Ca–O, La–O, and Mn–O from the absolute values of the binding energy difference (ΔBE) of Ca $2p$–O $1s$, La $3d$–O $1s$, and Mn $2p$–O $1s$ (*7, 8*). Figure 3 shows the XPS spectra of the Mg $2s_{1/2}$ and Mn $2p_{3/2}$ levels of $(Mg_{6-x}Al_x)MnO_8$. The binding energies of Mg $2s_{1/2}$, Mn $2p_{3/2}$, and O $1s_{1/2}$ are independent of the composition: 88.4 ± 0.1 eV for Mg $2s_{1/2}$, 643.0 ± 0.2 eV for Mn $2p_{3/2}$, and 530.2 ± 0.2 eV for O $1s_{1/2}$. In $(Mg_{6-x}Al_x)MnO_8$, there are two types of chemical bonding: Mg–O–(Al, Mg) and Mg–O–Mn–O–(Al, Mg). As the occupation rate of Al^{3+} ions at Mg^{2+} ion sites is less than 5%, the binding energy of Mg $2s_{1/2}$ in the chemical bonding of Mg–O–(Al, Mg) is not strongly affected by the Al^{3+} ion. According to Carver *et al.*, the binding energies of Mn $2p_{3/2}$ for MnI_2, $MnBr_2$, $MnCl_2$, MnF_2, MnS, and MnO are 642.1, 642.2, 642.1, 642.8, 640.5, and 641.7 eV, respectively (*9*). From these values, obviously the binding energy of Mn $2p_{3/2}$ for Mn–A_2 or Mn–A (A = halogen or chalcogen) increases with the increasing electronegativity of A. On the other hand, the binding energy of Mn $2p_{3/2}$ decreases with the decreasing valence of Mn ions; the binding energies of Mn $2p_{3/2}$ for $Mn^{4+}O_2$, $Mn^{3+}{}_2O_3$, and $Mn^{2+}O$ are 642.4, 641.8, and 641.7 eV, respectively (*9*). In the chemical bonding of Mg–O–Mn–O–(Al, Mg) in $(Mg_{6-x}Al_x)MnO_8$, the electronegativity of Al is larger than that of Mg (*10*). With increasing x, though the binding energy of Mn $2p_{3/2}$ in a part of the Mn ions increases owing to the high electronegativity of Al, the binding energy of Mn $2p_{3/2}$ in the rest of the Mn ions decreases owing to the Mn^{3+} ion. Consequently, the binding energy of Mn $2p_{3/2}$ cancels and is independent of the composition.

The full width at half maximum of the Mg $2s_{1/2}$ peak as shown in Fig. 3 is ca. 2.30 eV and independent of x. With increasing x, however, the FWHM of Mn $2p_{3/2}$ increases from 3.12 to 3.37 eV. From the magnetic measurement, the Mn^{3+} ion has both high-spin and low-spin states. However, the Mn $2p_{3/2}$ peak is broad and asymmetric as shown in Fig. 3. According to Kowalczyk *et al.*, the Mn $2p_{3/2}$ peak in MnF_2 is broad and asymmetric toward the high binding energy site, and this asymmetry was discussed in terms of multiples splitting (*11*). From these results, the increase of the FWHM of Mn $2p_{3/2}$ is explained by the presence of both the low-spin and high-spin states of the Mn^{3+} ion, or by canceling the binding energy of Mn $2p_{3/2}$. However, we could not identify the binding energy of the high-spin or low-spin state of the Mn^{3+} ion from the Mn $2p_{3/2}$ peak.

It is concluded that $(Mg_{6-x}Al_x)MnO_8$ ($0 \leq x \leq 0.3$) was synthesized at 1073 K using the solid state reaction. The cell constants of $(Mg_{6-x}Al_x)MnO_8$ monotonously decrease with increasing x. This decrease depends on the difference of the rate of increase for the ionic radii of the Mg and Mn sites. From the results of the magnetic measurement, the low-spin and high-spin states of the Mn^{3+} ions coexist. Though the binding energy of Mn $2p_{3/2}$ is indepndent of x, the FWHM of the Mn $2p_{3/2}$ peak increases with increasing x. The presence of both the low-spin and high-spin states of the Mn^{3+} ion causes an increase of the FWHM of the Mn $2p_{3/2}$ peak.

References

1. J. S. Kasper, and J. S. Prener, *Acta. Crystallogr.* **7,** 246 (1954).
2. P. Porta and M. Valigi, *J. Solid State Chem.* **6,** 34 (1973).
3. H. Taguchi and M. Nagao, *J. Mater. Sci. Lett.* **10,** 658 (1991).
4. A. Cimino and V. Indovina, *J. Catal.* **17,** 54 (1970).
5. R. D. Shannon and C. T. Prewitt, *Acta Crystallogr. Sect. B* **33,** 1299 (1977).

6. P. M. RACCAH AND J. B. GOODENOUGH, *Phys. Rev.* **155,** 932 (1967).
7. H. TAGUCHI AND M. SHIMADA, *Phys. Status Solidi B* **131,** K59 (1985).
8. H. TAGUCHI AND M. SHIMADA, *J. Solid State Chem.* **67,** 37 (1987).
9. J. C. CARVER, G. K. SCHERITZER, AND T. A. CARLSON, *J. Chem. Phys.* **57,** 973 (1972).
10. L. PAULING, "The Nature of the Chemical Bond," 3rd ed., Cornell Univ. Press, New York (1960).
11. S. P. KOWALCZYK, L. LEY, F. R. MCFEELY, AND D. A. SHIRLEY, *Phys. Rev. B* **11,** 1721 (1975).